Recovery of Tungsten Surface with Fiber-Form Nanostructure by the Effect of Surface Temperature Increase in Plasmas

Takanori MIYAMOTO†, Shuichi TAKAMURA†

Abstract One of the serious concerns for tungsten materials in fusion devices is the radiation defects caused by helium plasma irradiation since helium is the fusion product. Fiber-formed nanostructure is thought to have a possible weakness against the plasma heat flux and may destroy the reflectivity as an optical mirror. In this paper an interesting method for a recovery of such tungsten surfaces is shown.

1. Introduction

Divertor materials in fusion devices are exposed to high density and high heat flux plasmas. Tungsten(W) may be employed in the ITER because of its high thermal property and low sputtering yield. Moreover, tungsten is considered as a candidate for in-vessel mirror materials for optical diagnostic systems in ITER. However, it is known to be damaged by helium ion irradiation, and it is called helium defects. We have two kinds of helium defects. One is bubble/holes on the surface generated at relatively high surface temperature range more than about 1600K, associated by the ion bombarding energy larger than 6eV. The well-developed bubble/holes reaches several microns in size [1, 2]. The other is fiber-form nanostructure on the surface produced at relatively low temperature, less than 1500K [3, 4] and at the incident ion energy of greater than roughly 10eV [5]. The thickness of fiber is thin, typically several tens nanometer.

The surface characteristics of nanostructured W would change compared with the flat non-damaged surface, especially the heat conduction [6]. The damaged surface could be thought to have a weakness against the plasma heat flux. Thin fiber-form nanostructure would not be favorable for protecting the tungsten surface from a possible melting. Therefore, a recovery of tungsten surface with fiber-form nanostructure is crucial for heat and particle control in future fusion reactors. From the point of view of unipolar arcing [7], it is preferable to have a flat tungsten surface than the nanostructured one which is thought to give substantial thermoelectron emission through the tip of the fiber.

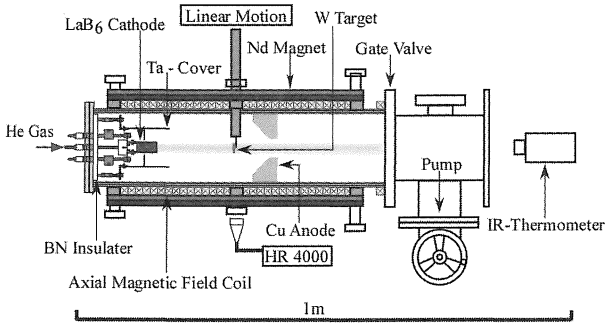

Fig.1 Experimental device – AIP-PID.

2. Experimental set-up and surface temperature estimation

The device for the present study is called AIT-PID (Aichi Institute of Technology – Plasma Irradiation Device) and has a machine structure shown in Fig.1. It is equipped with three

† 愛知工業大学　工学部　電気学科（豊田市）

pairs of neodymium permanent magnet bars (the cross section : 15×15mm) composing a multi-cusp (azimuthal mode number : 6) magnetic configuration. In addition a solenoidal winding underneath the magnets produces a weak axial magnetic field up to 10mT [8].

Figure 2 shows the fiber-form nanostructured tungsten made in AIT-PID where we have high density ($\sim 10^{18} m^{-3}$) helium plasma with the ion bombardment energy of 50eV and the starting surface temperature of 1420K [8, 9]. The helium ion fluence is $\sim 10^{26} m^{-2}$. The specimen is a cold worked powder metallurgy tungsten. One of the outstanding characteristics of AIT-PID is the presence of hot electron component (T_h ~30eV, α ~5%) where T_h and α are the temperature and the fraction of hot component while the bulk electron temperature is around 4eV.

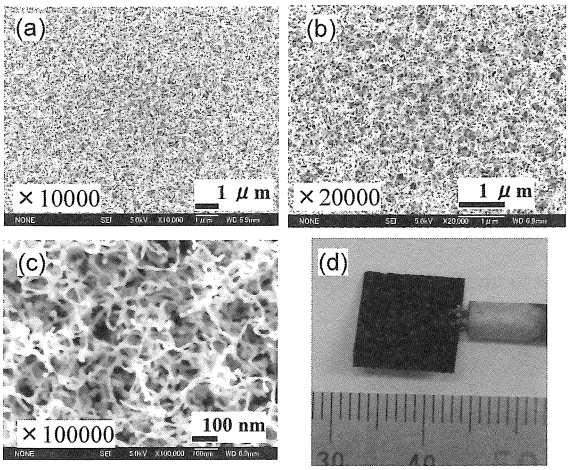

Fig.2 Fiber-form nanostructured tungsten surface due to helium plasma bombardment by AIT-PID. (a)~(c) are obtained with FE-SEM, and (d) is a photo of tungsten target with a support.

Figure 3 shows the time evolution of tungsten surface temperature monitored with IR (Infra Red) radiation thermometer with the measured wavelength of 0.9μm, silicon detector and the radiation emissivity of ε = 0.43 which is fixed during the exposure. At the end of irradiation the surface color is changed from originally silver to complete black, which suggests the emissivity increase from 0.43 up to almost 1.0. It means that the tungsten surface becomes an almost ideal black-body. We had an apparent dramatic decrement roughly 300K with this thermometer when the nanostructure is formed on the surface. We believe that the starting temperature obtained with radiation thermometer is correct since the appropriate emissivity is employed. The final temperature is estimated according to Planck's law as follows,

$$I(\lambda, T) = \frac{2hc^2\varepsilon}{\lambda^5} \frac{1}{e^{\frac{hc}{\lambda kT}} - 1} . \quad (1)$$

High frequency approximation $hc/\lambda kT \gg 1$ of Planck's formula gives the following simple equation with c = 3.0×10^8m/s, h = 6.63×10^{-34} m^2 kg / s and λ=0.9μm,

$$I(\lambda, T) = \frac{2hc^2\varepsilon}{\lambda^5} e^{-\frac{hc}{\lambda kT}} = A\varepsilon e^{-\frac{1.6\times10^4}{T[K]}} . \quad (2)$$

We examine what is the temperature difference ΔT measured with ε=0.43 and 1.0 at the final stage. We put $T_{1.0}$ and $T_{0.43}$ for estimated temperatures with the emissivities set at ε = 1.0 and ε = 0.43, respectively. Then we can derive an approximate formulae for the temperature difference with the same radiation intensity,

$$\Delta T = T_{1.0} - T_{0.43} = -0.84 \frac{\bar{T}^2}{1.60\times10^4} , \quad (3)$$

where $\bar{T}(=\sqrt{T_{1.0} \times T_{0.43}})$ is the effective average temperature.

Under the condition shown in Fig.3, we have $\bar{T}$~1200K, and ΔT=76K is obtained from eq.(3) so that the final temperature is estimated to be 1190K. In this run, the reduction of surface temperature is 260K.

In order to confirm the estimation of ΔT, we repeat a similar try. An another run of experiment where the starting temperature is 1455K gives the final temperature of 1158K with ε= 0.43 while the temperature of 1086K with ε=1.0 experimentally. Therefore, the ΔT obtained with IR thermometer is 72K. On the other hand, eq.(3) gives 64K for $\bar{T}$~1100K. These two values for ΔT is fairly close.

By the series of experiment for nanostructure formation on the W surface, we can say at least a substantial cooling occurs on the way to a blacking of the surface. The physical mechanism of cooling comes not only from the increase in radiation emissivity but also from a reduction in plasma heat flux on the surface through the sheath. The latter is brought in the present case by a deepening of floating potential due to a suppression of secondary electron emission from tungsten surface [10]. The flat tungsten surface may emit secondary electrons owing to a hot electron component which decreases the floating potential. The forest made of fiber-form nanostructure developed on the tungsten surface may inhibit the emission of secondary electrons to the surrounding plasma. Therefore, the energy transmission factor through the sheath is important when the plasma contains hot electron component [11].

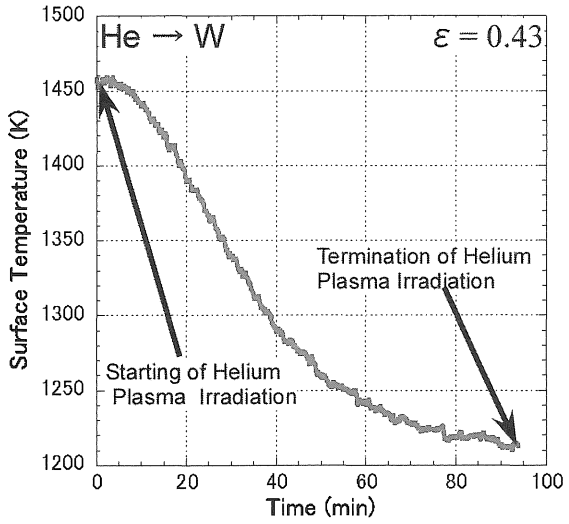

Fig.3 Temperature evolution of tungsten surface during helium plasma irradiation with the ion energy of 45eV.

3. Recovery of tungsten surface

The previous experiment of temperature excursion for nanostructured tungsten in the helium plasma [9] has already shown a shortening and a fattening of originally long and thin fibers when the surface temperature increases up to 1600K for a few minutes with an helium ion energy of larger than 6eV [12]. However, the holes and bubbles on the surface [8, 9] are newly created or survived so that a surface roughness may not be removed when the incident helium ion energy is larger than 6eV. It suggests that the recovery would be obtained with non-damage working gases like argon or helium plasma whose ion bombarding energy is of less than 6eV by increasing the electron heat load on fiber-form nanostructured surface. It is a kind of annealing technique using the plasma electron heat flux.

As the first step, a black tungsten plate with fiber-form nanostructure is exposed to a high density argon plasma. The ion bombarding energy corresponding to the sheath voltage is chosen to be 7eV avoiding any sputtering since the threshold energy is ~30eV, and the apparent surface temperature is set around 1700K, initially. The history of surface temperature is shown in Fig.4. In the course of measurement the emissivity is fixed at ε=0.43 for the infra-red emission of 0.9μm. A gradual increase in the surface temperature has been observed since a

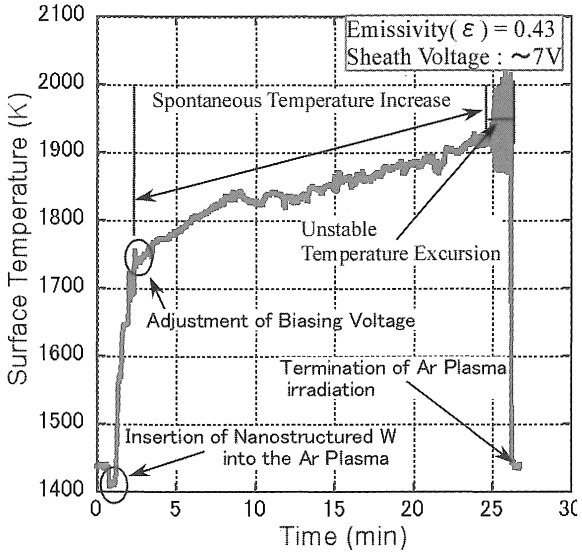

Fig.4 Time history of apparent tungsten surface temperature on the way to recovery of flatness with an exposure to argon plasma. The emissivity for radiation thermometer is fixed at ε=0.43. At the beginning, a fine adjustment of biasing gives a fairly large change in electron heat flux, which is reflected at the surface temperature.

decrease in emissivity brings a decrease in radiation loss with the same plasma heat load. In this case, we believe that the final temperature would be correct, while the starting temperature may be estimated by using eq.(3), roughly 100K lower.

Figure 5 shows some typical FE-SEM images of recovered tungsten surface after 25min irradiation of argon plasma. The apparent surfaces have a silver like metallic color as show Fig.5 (d). FE-SEM images show that any new bubble/holes are not formed on the surfaces but short fibers with sub-microns in length still exist on the surfaces. Some fiber roots whose size is a few hundred nanometer in thickness are observable in Fig.5 (b), while Fig.5 (c) shows that the height of fiber roots is around 100nm. Shortening and fattening of nano-fiber is confirmed with the irradiation of high heat flux argon plasma at a high surface temperature.

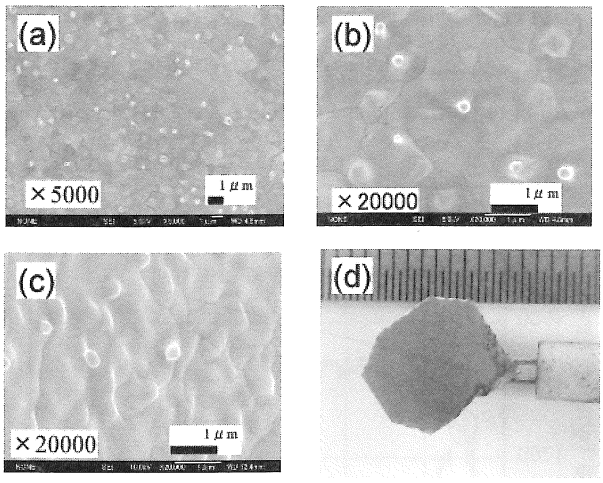

Fig.5 Surface morphology and photo for tungsten surface recovered by argon plasma irradiation. (a)~(c) are obtained with FE-SEM while (c) shows a grazing view, and (d) is a photo of tungsten target with a support.

As already pointed out, helium ions with the incident energy of less than 6eV cannot penetrate deep into the tungsten material since these ions cannot overcome the surface potential barrier [10], so that they do not produce any defects on the surface. Under such ion energy range, the nano-fibers are shortened and fattened without generating any new hole/bubble when increased heat load on the damaged black surface. The history of apparent surface temperature for this second step is now shown in Fig.6 where the incident ion energy is around 5eV. The starting surface temperature is adjusted at around 1700K. A spontaneous temperature increase may come from a

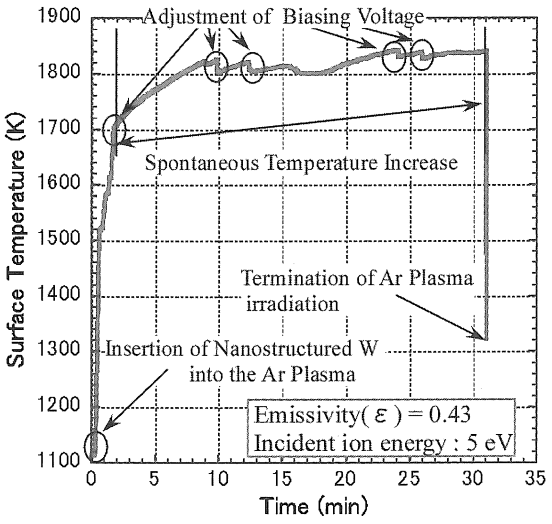

Fig.6 Time history of apparent tungsten surface temperature on the way to recovery of flatness with helium plasma. The emissivity for radiation thermometer is fixed at ε=0.43.

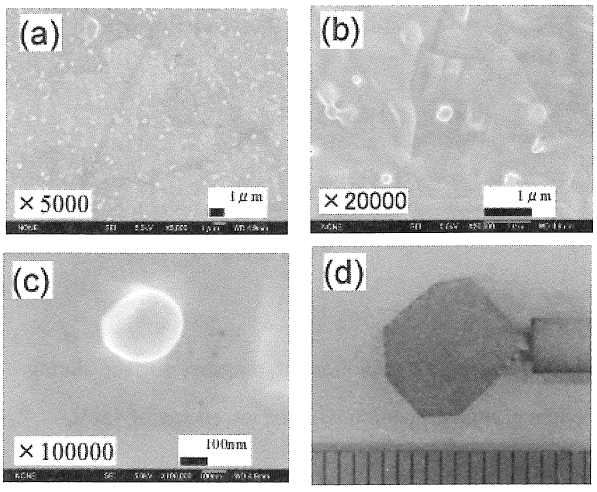

Fig.7 Surface morphology and photo for tungsten surface recovered by helium plasma irradiation. (a)~(c) are obtained with FE-SEM, and (d) is a photo of tungsten target with a support covered with a ceramic tube.

reduction of radiation emissivity, similarly to the previous recovery experiment shown in Fig.4. In order to avoid an overheating, the biasing voltage for tungsten was slightly increased at 4 times with a step of 0.1 V since the electron heat flux is very sensitive to the sheath voltage in this biasing range.

Figure 7 shows some typical FE-SEM images after 30min irradiation of helium plasma. The color of tungsten surface becomes silver metallic white, and FE-SEM images does not show any new bubble/holes formed on the surfaces but sub-micron fiber is still on the surfaces. Figure 7 (c) shows remaining fiber roots. These results are very similar to the results obtained by the irradiation of argon plasma.

Figure 8 shows some typical FE-SEM images after 60min irradiation of helium plasma, twice as long as in the previous case shown in Figs. 7 and 9. These images show a substantial diminution of fiber roots. Therefore, it is thought that almost complete recovery of nanostructured tungsten may be possible by a sufficiently long irradiation of helium plasma with a high surface temperature.

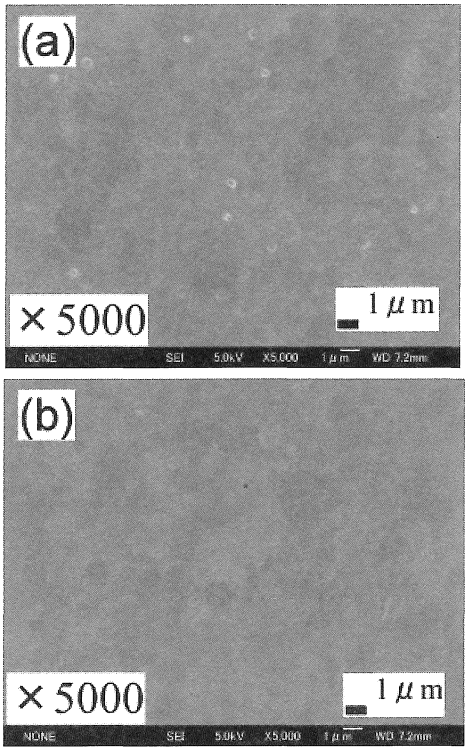

Fig.8 Surface morphology for the tungsten surfaces at different locations recovered by 60min helium plasma irradiation. (a) corresponds to a near-edge region, while (b) does to a central area of the specimen.

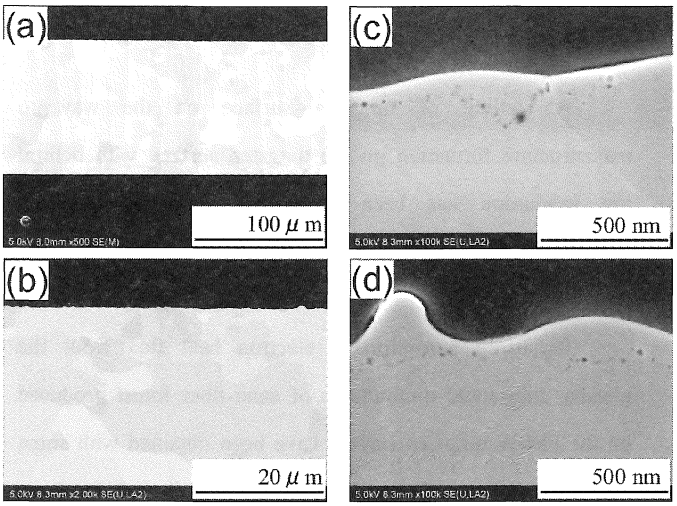

Fig.9 SEM photos of the cross-section of tungsten specomen which was recovered by the helium plasma flux from the helium defect fiber-form nanostructure.

4. Observation of cross – section

It is very important and curious to know what is the structure below the tungsten surface specimen. This is preformed for the recovered tungsten shown in Fig.7 with CP (Cross–section Polisher) technique using Ar ion beam (6 kV, 150μA). Figure 9 shows a few SEM images of the cross-section for the specimen shown in Fig.7. A wavy structure with the vertical scale of a few hundreds nanometers remain on the surface. A tiny bubble layer located roughly a hundred nanometer below the surface is found. The scale height of hundreds nanometer on the wavy surface is much smaller than the sheath thickness on the surface which is $7\lambda_{De}$ ~100μm with T_e ~4eV and n_e ~$10^{18}m^{-3}$.

We understand that such a wavy structure and a bubble layer would diminish if time for surface recovery would be long with a sufficiently high surface temperature.

5. Summary

A cooling of tungsten surface on the way to nanostructure formation on the tungsten surface with helium ion irradiation has been confirmed with the radiation thermometer associated by a simplified formula of Planck's law.

By using non-intrusive electron heat flux from the plasma, substantial diminutions of nano-fiber forest produced on the PM-W tungsten surface have been obtained with some short remains of fiber roots and a small bubble layer underneath the surface. The diminution of nano-fibers depends on the surface temperature and irradiation time. Complete recovery of tungsten without any remains like roots would be obtained with higher heat load or for longer exposure time. On the way of recovery any serious tungsten contamination was not detected. The above procedure could be one of healing technique for tungsten surface with helium defects.

Acknowledgment

The work is supported by a Grant-in-aid for scientific Research (B) (20360414) from JSPS. The authors would like to thank Prof. N. Ohno and Dr. S. Kajita of Nagoya University for their discussions, and Assoc. Prof. H. Iwata for his help on FE-SEM manipulation.

References

[1] M.Y. Ye, S. Takamura and N.Ohno, J. Nucl. Mater. **241-243** (1997) 1243.

[2] S. Takamura, Plasma Fusion Res. **81** (2005) 25 (in Japanese).

[3] S. Takamura, N. Ohno, D. Nishijima and S. Kajita, Plasma Fusion Res. **1** (2006) 051.

[4] M.J. Baldwin and D.P. Doener, Nucl. Fusion **48** (2008) 035001.

[5] W. Sakaguchi, S. Kajita, N. Ohno and M. Takagi, J. Nucl. Mater. **290-291** (2009) 1149.

[6] S. Kajita, S. Takamura, N. Ohno, D. Nshijima, H. Iwakiri and N. Yoshida, Nucl. Fusion **47** (2007) 1358.

[7] S. Kajita, S. Takamura and N. Ohno, Nucl Fusion **49** (2009) 032002.

[8] S. Takamura, T. Tsujikawa, Y. Tomida, K. Suzuki, T. Minagawa, T. Miyamoto and N. Ohno, J. Plasma Fusion Res. SERIES **9** (2010) 441.

[9] S. Takamura et al., J. Nucl. Mater. (2011), doi: 10.1016/j.jnucmat.2010.12.021.

[10] S. Takamura, T. Miyamoto, Plasma Fusion Res. **6** (2011) 005.

[11] S. Masuzaki, N. Ohno and S. Takamura, J. Nucl. Mater. **223** (1995) 286.

[12] D. Nishijima, M.Y. Ye, N. Ohno and S. Takamura, J. Nucl. Mater. **329-333** (2004) 1029.